J Solid State Electrochem (2003) 7: 264–270
DOI 10.1007/s10008-002-0335-y

ORIGINAL PAPER

M. Miranda-Hernández · J.A. Ayala
Marina E. Rincón

Electrochemical storage of hydrogen in nanocarbon materials: electrochemical characterization of carbon black matrices

Received: 6 June 2002 / Accepted: 9 October 2002 / Published online: 6 November 2002

Abstract In this work, various types of carbon black are electrochemically characterized to study their possible use in the electrochemical evaluation of fullerene materials as hydrogen storage candidates. The cyclic voltammetry and chronopotentiometry studies were performed in alkaline media, 6 M KOH, with carbon paste electrodes. Differences in the electrodes' electrochemical response and their correlation with the various surface chemistries, morphology and doping species of carbon blacks suggest a stronger dependency on the presence of doping agents (foreign metals) and on the surface structure than on the carbon black surface area. The study allows the selection of appropriate carbon black materials to be used as matrixes in future fullerene composite studies.

Keywords Carbon black · Carbon paste · Cyclic voltammetry · Hydrogen storage

Introduction

Hydrogen is the cleanest, sustainable and renewable energy carrier, and a hydrogen energy system is expected to progressively replace the existing fossil fuels in the future [1]. Thus, the safe storage of hydrogen is critical to hydrogen/air fuel cells or hydrogen-driven combustion engines in vehicles. The available storage technologies today (cryogenic liquid hydrogen, compressed gas storage, or metal hydride storage technology) are not capable of meeting the goal set by the US Department of Energy (DOE) of 6.5 wt% hydrogen and a volumetric density of 62 kg H_2/m^3 [2, 3, 4]. Intensive research on light metal hydrides [5, 6, 7, 8, 9, 10, 11, 12] continues, while the interest in the potential of carbon materials as hydrogen storage media has undergone a resurgence following the claims that single-wall carbon nanotubes and certain types of vapor-grown carbon fibers may have high hydrogen-storage capacities at room temperature [2, 3, 4, 13, 14, 15, 16, 17].

In the hydrogen uptake studies, carbon materials have been used as composite electrodes in the form of pellets, paste or films. The composite electrode typically consists of a matrix (carbon black, graphite, polymer or metals) and carbon nanotubes or nanofibers as the active material. Among the advantages of using a carbon matrix are its low weight and cost, plus the extensive variety of carbons that are available with a wide range of physicochemical properties. In particular, the use of carbon black as a matrix material in the electrochemical evaluation of carbon nanotubes relies on the fact that hydrogen uptake is proportional to its surface area and pore volume, and requires very low temperatures such as liquid nitrogen temperature. This physisorption of H_2 is assumed negligible on carbon black at room temperature and atmospheric pressure. In fact, the highest volumetric storage capacity of commercially available activated carbon, with an area much larger than carbon black, is around 32 kg H_2/m^3 at 77 K and 50 bar [2].

The great deal of controversy [4, 18, 19] on the hydrogen storage capacity of carbon nanotubes and graphite nanofibers indicates that, up to now, not all the variables have been systematically studied. In general, there is a large skepticism about the high-pressure sorption studies at room temperature, where experimental errors have been suggested to explain claims of hydrogen uptake better than 1 wt% [19]. On the other hand, the possible contamination of carbon nanotubes with metals has been cited as the source of irreproducible data among different research laboratories [20]. Currently, it is well accepted that there is a need for comparative investigations at different laboratories on

Presented at the XVII Congress of the Mexican Electrochemical Society, 26–31 May 2002, Monterrey, Mexico

M. Miranda-Hernández · M.E. Rincón (✉)
Centro de Investigación en Energía-UNAM,
Apartado Postal 34, Temixco, Morelos 62580, Mexico
E-mail: merg@cie.unam.mx
Tel.: +52-555-6229748

J.A. Ayala
Columbian Chemicals Co.,
1800 West Oak Commons Ct., Marietta, GA 30062, USA

the same sample or comparative investigations with the same measurement method [1].

Even though the electrochemical method is easier and faster than the high-pressure method to evaluate the hydrogen storage capacity of fullerenes, few reports [14, 15, 16] exist in the literature in this respect, and in all of them the electrode is a combination of metals (Cu, Au, Pd, Ni) and carbon nanotubes. Our skepticism arises from the choice of metals, whose hydrogen uptake is well documented [5, 6, 7, 8, 9, 10, 11, 12]. In this work, we study the electrochemical response of various types of carbon black under conditions similar to those reported for the electrochemical evaluation of carbon nanotubes, with the aim of using them as the matrix material instead of the metals commonly used. Understanding the relationship between the physicochemical properties and the electrocatalytic properties of carbon is necessary to optimize the utilization of carbon electrodes in hydrogen storage or in the electrochemical hydrogen storage evaluation of nanotubes. Cyclic voltammetry and chronopotentiometry were used to gather the electrochemical data reported here.

Experimental

Electrochemical measurements were carried out with Basic Autolab W/PGSTAT30&FRA equipment, in a conventional three-electrode cell consisting of a working carbon paste electrode, a graphite counter electrode and a Hg/HgO/1 M KOH reference electrode (+0.2 V vs. NHE). The aqueous electrolyte was 6 M KOH and both reference and counter electrodes were kept in separate compartments. Carbon blacks supplied by Columbian Chemical from four different experimental trials were characterized: C-NSMT, C-SMT, C-LIMT and C-MA21. As a reference, a commercial carbon black (C-Black) was also characterized. Table 1 presents some of the characteristics of these carbon blacks. The major difference between C-SMT and C-LIMT is that the latter has been doped with lithium and has a lower amount of sulfur. Carbon paste electrodes were prepared by mixing carbon black (CB) and silicon oil (S) with the weight ratio of CB:S = 80:20, except for the material labeled C-MA21, where an inverted weight ratio of 20:80 was required owing to the significantly higher surface area and structure of this carbon black when compared to C-NSMT, C-SMT and C-LIMT. In all the electrodes the consistency of the paste was equivalent. A unique ratio was not possible since the 80:20 ratio was insufficient for C-MA21 (too powdery), and the 20:80 ratio was excessive for the other carbons (too liquid).

Once the consistency of the paste was right, it was supported in a 0.4 mm thickness Teflon ring (0.96 cm^2), with stainless steel as the back contact. All the experiments took place under stationary conditions, with nitrogen being bubbled through the electrolyte prior to and between all measurements. Moreover, nitrogen was kept flowing over the solution during the measurements. In each case the bulk resistivity of the paste was monitored against the ferro/ferricyanide reaction. Here, cyclic voltammetry studies were performed on an electrolyte solution containing 0.01 M ferro/ferricyanide and 1 M KCl. Regardless of the different CB/S ratio, all carbon paste electrodes reproduced reasonably well the typical electrochemical response of this redox couple. This confirms that percolation is reached in all cases, and that all carbon paste electrodes have approximately the same bulk resistivity. Additionally, to assure similar interfacial conditions and good reproducibility, each experiment was run with a renewed surface.

Cyclic voltammetry studies in alkaline media were performed in the potential range of 0.6 V to –1.5 V vs. Hg/HgO/1 M KOH. The sweep initiated at rest potential (V_r) in the negative direction and with a scan rate of 50 mV/s. A constant double current pulse (±) was used for the chronopotentiometry studies, and their magnitude depended on the type of carbon black.

Results

Figure 1 compares the cyclic voltammograms (first cycle) of the various types of carbon black, recorded at 50 mV/s in the potential window of 0.5/0.8 V to –1.6 V vs. Hg/HgO. It can be observed that the current response depends on the type of material, and that an inflexion (c_0) and two cathodic peaks (c_1, c_2) appear during the potential swept in the negative direction. The separation between c_0/c_1 and between c_1/c_2 is ~0.5 V and ~0.4 V, respectively. The inflexion (c_0) occurs at –0.1/–0.3 V vs. Hg/HgO in all carbon blacks except for C-MA21. In this material, negligible current is observed at potentials more positive than –0.4 V vs. Hg/HgO. All the materials present the cathodic peak (c_1) around –0.7/–1.0 V vs. Hg/HgO; the least and most negative values correspond to C-LIMT and C-MA21, respectively. With regard to the cathodic peak (c_2), it is absent for C-LIMT and C-NSMT, while it appears around –1.4 V vs. Hg/HgO for C-MA21 and at –1.2 V for C-SMT and C-Black. Additionally, at the outermost negative potential, all the electrodes show a fast increase in current associated with the hydrogen evolution reaction. During the inversion of the potential swept, the presence of anodic peaks (a_1, a_2) are well known in the response of C-SMT and C-LIMT, while weaker faradic and capacitive anodic currents, with substantial voltage delay, are typical of C-NSMT, C-MA21 and C-Black.

Cyclic voltammograms were also obtained without regenerating the carbon surface during five cycles. These are shown in Fig. 2, where at intermediate potentials an increase in cathodic/anodic current is observed for C-SMT (Fig. 2a) and C-LIMT (Fig. 2b). Additionally, at the outermost negative potential these materials show a decrease in cathodic current with cycling, which indicates a higher overpotential for hydrogen evolution. During

Table 1 Morphology parameters and chemical composition of carbon blacks

Sample	Mean particle size (nm)	BET surface area (m^2/g)	DBPA[a] (mL/100 g)	Sulfur (%)	Lithium (ppm)
C-SMT	390	6.6	42	0.35	< 1
C-NSMT	390	6.5	44	0.03	< 1
C-LIMT	390	5.5	42	0.02	700
C-MA21	25	80	170	0.01	–

[a]Dibutyl phthalate absorption

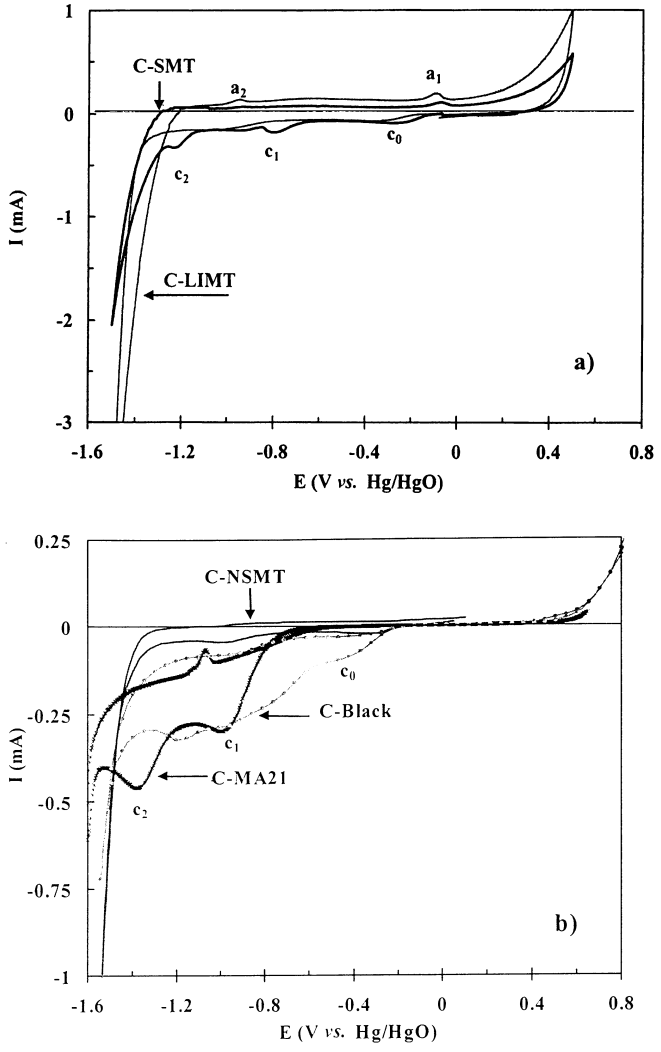

Fig. 1a, b Cyclic voltammograms (first cycle) for carbon paste electrodes based on different carbon blacks (see Table 1) in 6 M KOH and at 50 mV/s. All paste electrodes contain 0.1122 g of carbon black and have a geometric area of 0.96 cm^2

inversion at –1.5 V vs. Hg/HgO, C-SMT keeps its value of voltage delay regardless of the number of cycles, while C-LIMT shows an increase in voltage delay that substantially modifies the shape of the curve. In both materials, the redox processes (c_0, c_1, c_2, a_1, a_2) tend to disappear with cycling.

In contrast to the materials just described, the overall current response of C-NSMT (Fig. 2c) and C-MA21 (Fig. 2d) has either no correlation or tends to decrease with the number of cycles. In these electrodes the redox processes associated with c_0, c_1, c_2 and a_1 clearly decrease as the number of cycles increases, while a_2 remains nearly constant or even increases. The behavior of the anodic peak (a_2) is particularly different for C-MA21 from the other carbon blacks. In this material, a_2 substantially grows with cycling, as is evidenced in Fig. 3, where the first two cycles of C-MA21 are shown at different potential scan rates. The comparison with Fig. 2d indicates that some degree of hydrogen evolution is required for the a_2 peak to appear (compare the current at the outermost negative potential in Figs. 1b, 2d and 3).

With the purpose of evaluating the charge-discharge capacities of the various materials, Fig. 4 shows the voltage-time curves of C-LIMT during chronopotentiometry studies at a constant current of $\pm 6\times10^{-5}$ A: a 50 s direct pulse (–) and a 100 s inverse pulse (+). The time difference in both pulses was aimed at enhancing the basic properties of the carbon blacks during electrochemical oxidation (discussed later), and consequently its electrochemical and chemical hydrogen uptake. During the negative pulse, C-LIMT presents a gradual transition from a complex spectrum dominated by three electrochemical processes (first cycle: zones m_1, m_2 and m_3) to a spectrum in which only the electrochemical process m_1 dominates.

The voltage-time curves of C-MA21 were obtained during chronopotentiometry studies at a constant current of $\pm 6\times10^{-5}$ A (Fig. 5a) and $\pm 1.5\times10^{-4}$ A (Fig. 5b): a 100 s direct pulse (–) and a 200 s inverse pulse (+). At the lower perturbation current, C-MA21 starts at a potential more negative than C-LIMT and as the number of cycles increases this potential becomes less negative, in close resemblance to the low current behavior of the lithiated carbon black (i.e., the anodic pulse facilitates the cathodic process occurring around –0.4 V vs. Hg/HgO in C-LIMT, and around –0.7 V vs. Hg/HgO in C-MA21). On the other hand, at the more intense double current pulse (Fig. 5b), C-MA21 presents several electrochemical cathodic processes, with the most negative becoming dominant with cycling. This behavior indicates that most of the surface groups on carbon are relevant during the first cycles, but afterwards it is the direct interaction of carbon with the hydrogen-containing species of the electrolyte that dominates.

Discussion

The comparison of Figs. 1 and 2 suggests different electrochemical processes in the carbon blacks analyzed. Owing to the characteristics of the paste (i.e., a non-conducting binder), depletion of electroactive species in the solid is expected in all paste electrodes in the first two or three cycles. For the materials studied, most of the cathodic and anodic peaks correspond to the reduction and oxidation of surface oxide groups on carbon, whose asymmetry (irreversibility) causes their disappearance during cycling. The reduction of quinone and carbonyl groups have been reported to be at –500 mV and –1350 mV (SCE) in 0.1 M KCl, respectively [21]. On the other hand, corrosion of carbon in alkaline solution, taken into account carbonate ion formation, has been reported to be [21]:

$$C + 6OH^- \rightarrow CO_3^{2-} + 3H_2O + 4e^- \quad (1)$$

The standard electrode potential at 25 °C is –0.682 V (vs. a Hg/HgO reference electrode) in 0.1 M CO_3^{2-} at

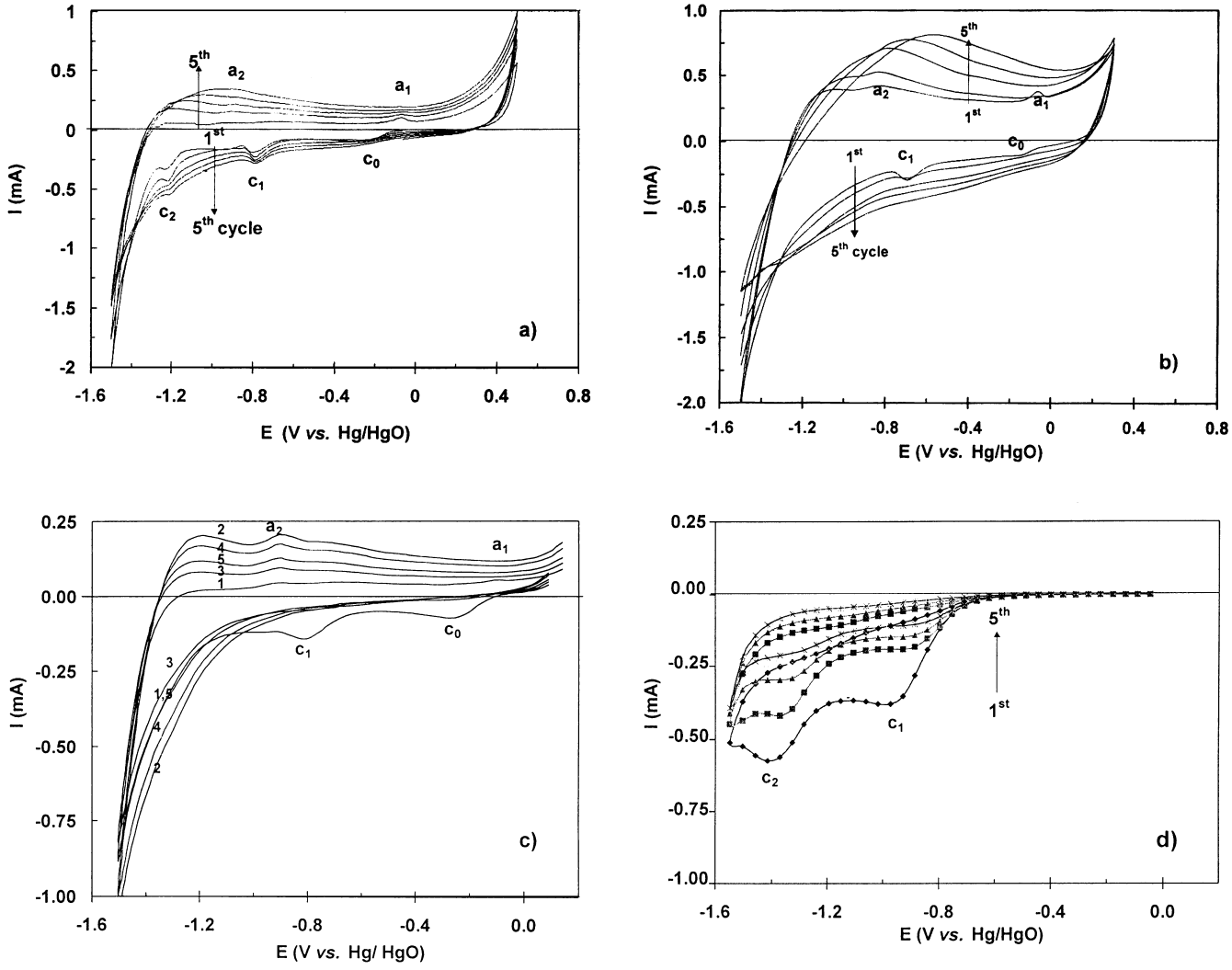

Fig. 2 Cyclic voltammograms (5 cycles) for: **a** C-SMT, **b** C- LIMT, **c** C-NSMT and **d** C-MA21. Curves obtained at 50 mV/s in 6 M KOH

pH 14, with the corrosion rate being determined by the surface structure of carbon. At potentials close to 0.5 V (vs. Hg/HgO), it occurs with the formation of CO, CO_2, surface oxides and organic carbon products, with the concurrent evolution of O_2. The last reaction becomes dominant at potentials above 0.5 V vs. Hg/HgO [22]. The morphological changes of porous carbon electrodes that are susceptible to corrosion in alkaline solutions involve the precipitation of alkali carbonate in the pores of carbon, so that carbon particles become electrochemically isolated and no longer corrode [21]. In addition, some authors have reported that the electrochemical surface treatment of carbon blacks in a potassium hydroxide solution increases its pH due to the formation of basic functional groups [23]. They elaborate that the basic groups are capable of complexing protons to its structure through the following equilibrium reaction with water:

$$C_{basic} + 2H_2O \rightarrow CH_3O^+ + OH^- \quad (2)$$

In our study, the influence of basic groups formed by electrochemical oxidation will be observed after the first cycle owing to the negative direction of the potential swept. Indeed, after the 3rd or 4th cycles the voltammograms present the typical capacitive response of adsorption processes, and at the 5th cycle the various carbon blacks strongly differ in the amount of current associated with double-layer charging, with the largest current associated with C-LIMT and the smallest current with C-MA21.

Taking into account that some of the chosen carbon blacks have been doped with metals and other elements, it is important to review the mechanism for evolution of hydrogen on metal surfaces. In alkaline electrolytes the overall hydrogen evolution reaction is represented by Eq. 3:

$$H_2O + e^- \rightarrow 0.5H_2 + OH^- \quad (3)$$

The detailed mechanism involves two electrochemical steps and one chemical reaction. Thus the hydrogen-containing species, once it reaches the electrode zone, can be converted electrochemically to an adsorbed hydrogen atom ($M + H_2O + e^- \rightarrow MH_{ads} + OH^-$), or it can

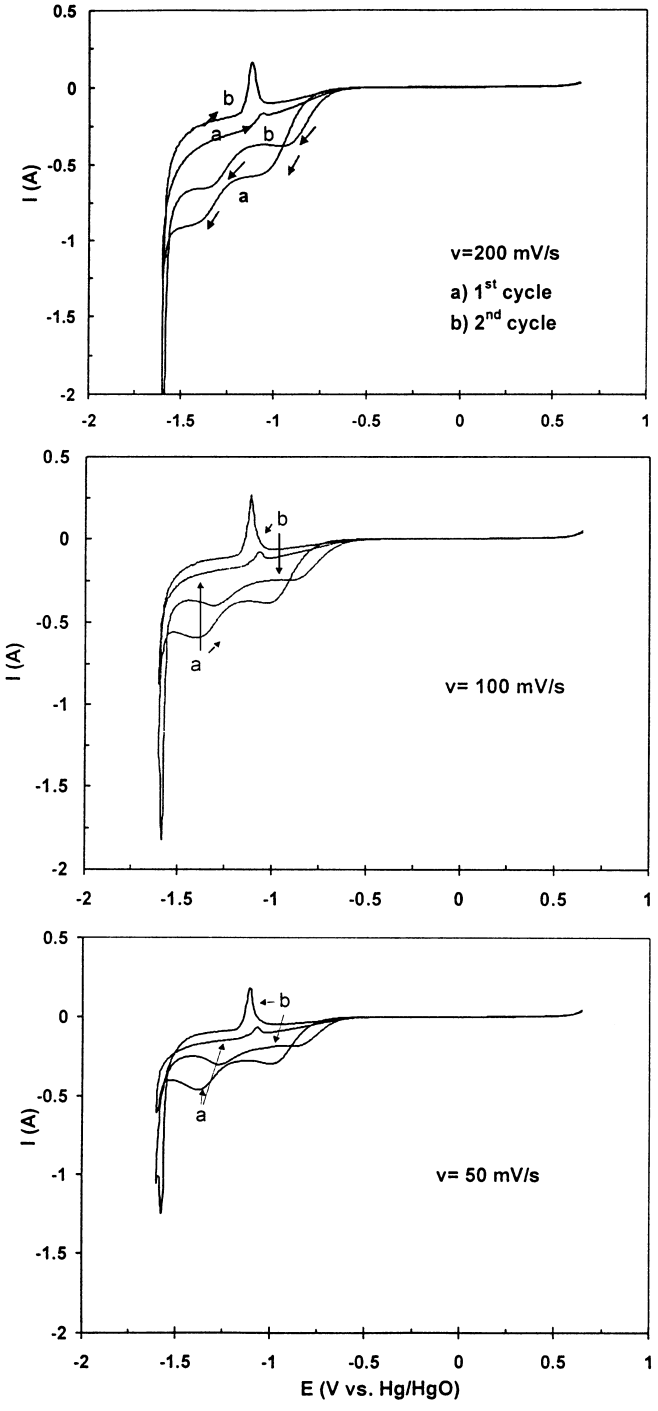

Fig. 3 Cyclic voltammograms (2 cycles) for carbon paste electrodes based on C-MA21. Curves obtained at different potential scans in 6 M KOH

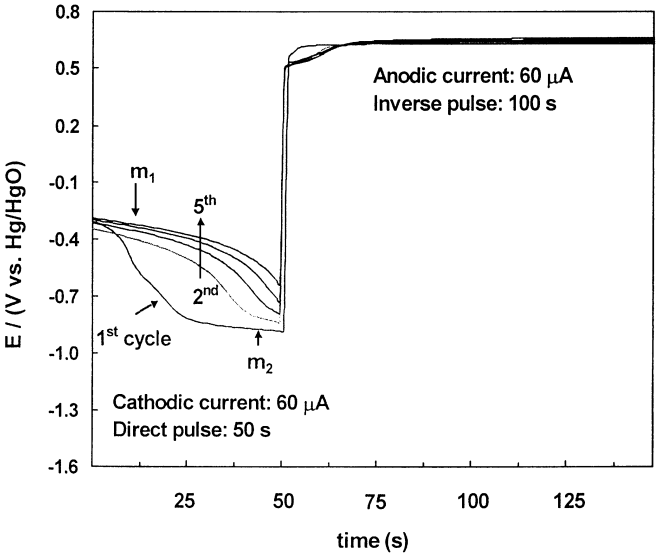

Fig. 4 Chronopotentiometry curves for C-LIMT in 6 M KOH. Double current pulse of $\pm 6\times10^{-5}$ A: a 50 s (direct pulse) and a 100 s (inverse pulse). Mass of carbon black: 0.1122 g; electrode geometric area: 0.96 cm^2

electrochemically react with other adsorbed species ($MH_{ads} + H_2O + e^- \rightarrow M + H_2 + OH^-$). The adsorbed hydrogen atoms can also react chemically to produce molecular hydrogen ($2MH_{ads} \rightarrow 2M + H_2$). These molecules leave the electrode by diffusion in the form of gas bubbles. The accepted mechanisms for hydrogen evolution on metal surfaces are the Volmer-Heyrovský mechanism and the Volmer-Tafel mechanism [7, 9, 23].

In the case of hydrogen evolution on carbon surfaces, two mechanisms are advanced [21]: (1) slow discharge/electrochemical desorption with a limited number of sites for hydrogen adsorption and (2) a coupled discharge/recombination reaction for hydrogen evolution. The first mechanism is equivalent to the two electrochemical steps suggested for hydrogen evolution on metal surfaces, while the second mechanism is equivalent to the first electrochemical step on metal electrodes followed by chemical recombination. Since the hydrogen overpotential on most carbon surfaces is high, it is expected that the doping agent will have a predominant role in doped carbon blacks.

The various potential responses (m_1, m_2, m_3) obtained in the chronopotentiometry studies, and the fact that they become less or more predominant with cycling, indicate that one of the processes is more irreversible and/or more disturbed during the anodic pulse. For C-LIMT, the behavior of the V vs. t curves agrees with the cyclic voltammogram shown in Fig. 2b, where the capacitive current of C-LIMT increases with the number of cycles in the potential range –0.3 V to –0.8 V vs. Hg/HgO, while the redox processes around –0.2 and –0.7 V vs. Hg/HgO tend to disappear. Reduction of adsorbed oxygen takes place at –0.26 V vs. Hg/HgO (through the peroxide pathway), and the electrochemical oxidation of carbon (anodic pulse) has been reported to be detrimental to it [21]. On the other hand, the electrochemical reduction of quinone and carboxyl groups could be competing with the chemical pathway depicted by Eq. 2. The steep voltage response of C-LIMT, observed when inverting the pulse in the chronopotentiometry studies, manifests the strong irreversibility of the cathodic processes assigned to c_0 and c_1.

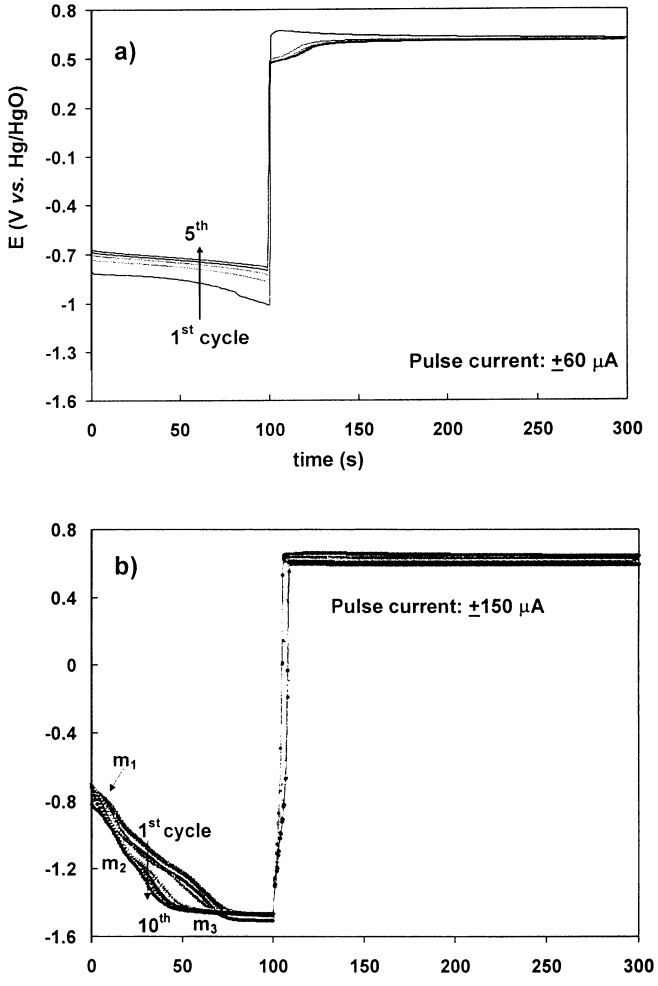

Fig. 5a, b Chronopotentiometry curves for C-MA21 in 6 M KOH. Double current pulse of: **a** $\pm 6\times10^{-5}$ A; **b** $\pm 1.5\times10^{-4}$ A. Direct pulse: 100 s, inverse pulse: 200 s. Mass of carbon black: 0.1122 g; electrode geometric area: 0.96 cm^2

It should be pointed out that larger current intensities (on the order of 10^{-4} A) could not be sustained for various cycles in carbon paste electrodes based on C-LIMT and C-SMT, since they degrade due to the hydrogen evolution reaction. On the contrary, the large overpotential of C-MA21 allows for chronopotentiometry studies with stronger perturbation currents. In this material, it is clear the appearance and/or enhancement with cycling of the process around –1 V vs. Hg/HgO. At this potential, the chronopotentiometry curves indicate some sort of reversibility (i.e., small voltage difference to sustain the double current pulse).

Strong similarities were expected (and indeed occur) between the chronopotentiometry curves of C-SMT and C-LIMT owing to the characteristics of their voltammograms (Fig. 2a vs. 2b). In the case of C-MA21, the voltammograms indicated a decrease in the pseudocapacitive response with the number of cycles, in contrast to the increase observed in C-LIMT (Fig. 2a vs. 2d). This decrement in double-layer charging explains the shift of the C-MA21 chronopotentiometry curves to more negative potentials.

Even though the different CB/S ratios of the electrodes based on C-MA21 could be a factor for its different electrochemical behavior, the experiments performed on the ferro/ferricyanide redox couple indicate otherwise. More relevant is the disordered and low structured nature of C-LIMT, which contrasts with the highly structured nature of C-MA21. The latter has its graphene sheets well aligned and parallel to the top surface due to the partial graphitization process occurring during the thermal treatment at which it is subjected (2200 °C in N_2). In addition, its larger surface combines to produce a material where hydrogen oxidation/desorption is more likely, resembling the reversible behavior reported for the electrochemical storage of hydrogen in carbon nanotubes [15, 16]. Graphitization is expected to enhance the kinetics of adsorption/desorption events since most of the electrochemical activity occurs on the exposed (outer) basal planes of carbon. In our studies, the smaller particle size of C-MA21 causes a large density of grain boundaries and very likely a large density of edge planes. This creates a situation in which the slow intercalation/adsorption at edge planes delays hydrogen evolution and allows for the inverse process to be observed in the reverse scan. The enhancement of this anodic signal with cycling indicates that activation and/or exfoliation of carbon is a requirement for efficient hydrogen oxidation/desorption reactions.

With regard to C-LIMT, its large particle size, low structure, large oxygen content, and the presence of lithium, combine to facilitate the kinetics of electrostatic adsorption/desorption processes (double-layer charging) and hydrogen uptake, without a clear presence of faradic reactions corresponding to hydrogen oxidation/desorption processes. The electrochemical response of this carbon is very different to the reported for carbon nanotubes, indicating that little interference would occur when used as a matrix. Carbon blacks (C-SMT and C-NSMT) with morphologies equivalent to C-LIMT, but with a different chemical composition, have a much lower capacitive current (particularly low anodic current), suggesting that double-layer charging is enhanced by lithium.

Conclusions

We present the results of the electrochemical characterization of various carbon blacks obtained by cyclic voltammetry and chronopotentiometry studies. The materials are intended to be used as matrices in the electrochemical evaluation of fullerenes as hydrogen storage materials. The features observed in the material labeled C-LIMT are considered to be most appropriate for that particular use: low structure and low surface area, which will not interfere with the electrochemical activity of carbon nanotubes. On the other hand, the similarities between the electrochemical response of

carbon nanotubes and the graphitic C-MA21 carbon black indicate that the latter could be considered as a candidate for the reversible electrochemical storage of hydrogen. The likely synergism between the graphitic carbon black matrix and fullerene will be the subject of future studies.

Acknowledgements The authors are grateful to the Electrochemical Laboratory of UAM-Iztapalapa for assistance with the electrochemical characterization of the materials, to Columbian Chemicals Company for the materials supplied, and to CONACyT-MEXICO for financial support.

References

1. Cheng HM, Yang QH, Liu C (2001) Carbon 39:1447
2. Yin YF, Mays T, McEnaney B (2000) Langmuir 16:10521
3. Dilon AC, Jones KM, Bekkedahl TA, Kiag CH, Bethune DS, Heben MJ (1997) Nature 386:377
4. Chambers A, Park C, Baker RTK, Rodriguez NM (1998) J Phys Chem B 102:4253E
5. Bernardini M, Comisso N, Davolio G, Mengoli G (1998) J Electroanal Chem 442:125
6. Czerwinski A, Kiersztyn I, Grden M (2000) J Electroanal Chem 492:128
7. Krstajic N, Popovic M, Grgur B, Vojnovic M, Sepa D (2001) J Electroanal Chem 512:16
8. Krstajic N, Popovic M, Grgur B, Vojnovic M, Sepa D (2001) J Electroanal Chem 512:27
9. Wang C (1998) J Electrochem Soc 145:1801
10. Ekdunge P, Jüttner K, Kreysa G, Kessler T, Ebert M, Lorenz WJ (1991) J Electrochem Soc 138:2660
11. Jaksic JM, Vojnovic MV, Krstajic NV (2000) Electrochim Acta 45:4151
12. Comisso N, Davolio G, Soragni E, Mengoli G (2001) J Electroanal Chem 512:92
13. Che G, Lakshmi BB, Fisher ER, Martin CR (1998) Nature 393:346
14. Nützenadel C, Züttel A, Chartouni D, Schlapbach L (1999) Electrochem Solid State Lett 2:30
15. Lee SM, Park KS, Choi YC, Park YS, Bok JM, Bae DJ, Nahm KS, Choi YG, Yu SC, Kim N, Frauenheim T, Lee YH (2000) Synth Met 113:209
16. Rajalakshmi N, Dhathathreyan KS, Govindaraj A, Satishkumar BC (2000) Electrochim Acta 45:4511
17. Che G, Lakshmi BB, Martin CR, Fisher ER (1999) Langmuir 15:750
18. Dresselhaus MS, Williams KA, Eklund PC (1999) MRS Bull 24:45
19. Tibbetts GG, Meisner GP, Olk CH (2001) Carbon 39:2291
20. Hirscher (2001) Appl Phys A 72:129
21. Kinoshita K (1988) Carbon: electrochemical and physicochemical properties. Wiley, New York
22. Ross PN, Sokol H (1984) J Electrochem Soc 131:1746
23. Park SJ, Kim JS (2001) Carbon 39:2011